

Calculation of soil water characteristic curve based on liquid bridge theory

Minpeng Tang¹, Dantong Lin² and Liming Hu³

¹PhD Student, State Key Laboratory of Hydro-Science and Engineering, Department of Hydraulic Engineering, Tsinghua University, Beijing, 100084, China, email: tmp22@mails.tsinghua.edu.cn

²Doctor, State Key Laboratory of Hydro-Science and Engineering, Department of Hydraulic Engineering, Tsinghua University, Beijing, 100084, China, email: ldt16@tsinghua.org.cn

³Professor, State Key Laboratory of Hydro-Science and Engineering, Department of Hydraulic Engineering, Tsinghua University, Beijing, 100084, China, email: gehu@tsinghua.edu.cn

ABSTRACT

Soil water characteristic curve (SWCC) is one of the most important characteristics of unsaturated soil. In most previous studies, the SWCC is obtained by fitting experimental results with numerical models such as the van Genuchten model, which depends heavily on the accuracy of the experimental data. In this study, the SWCC is interpreted and predicted directly based on the analysis of the liquid bridge. Two unequal-sized spheres are used to describe uneven-sized coarse particles, and the roughness on the surface of the particles is described by the spacing between them. The liquid bridge between these two particles is analysed based on the geometrical relationships. The influence of parameters including the relative size of the sphere, the relative interval of spheres and the liquid-solid contact angles on the normalized water content, matric suction and capillary force is discussed. Results show that water content increases with the increase of the relative size of spheres (from zero to one) or the decrease of the liquid-solid contact angle. This trend is more obvious when the relative size of spheres or the liquid-solid contact angle is small. If the relative interval of spheres cannot be ignored, there will be two water contents corresponding to the same matrix suction. One with smaller normalized water content is unstable, and the other with higher normalized water content is stable. The SWCCs of the compact cubic packing model are predicted based on the equal matrix suction assumption, which is compared to the prediction by existing theory.

Keywords: liquid bridge, unsaturated soil, soil water characteristic curve, capillary force, coarse sphere

1 INTRODUCTION

The soil water characteristic curve (SWCC) is one of the fundamental characteristics of soil, which can be used to explain and analyse infiltration, drainage, water and solute movement, and water availability. Previous studies have reported that the SWCC is affected by numerous factors, including water content, pore structure and the particle size of soil mass (Miller *et al.*, 2002), stress history (Ng *et al.*, 2000), dehydration and contact angle of air-water interface (Czachor *et al.* 2010), etc.

In previous studies, SWCC data measured by the negative pressure meter, tensiometer and other instruments can be fitted into a continuous function through mathematical models, such as the vG (van Genuchten) model (van Genuchten M.T., 1980). This method is widely used in research and engineering. However, measuring SWCC data takes a long time and the SWCC fitted by the tested data is affected by the sampling error. In addition, the physical meaning of the fitted mathematical model parameters is unclear.

The other method is to predict the SWCC directly from numerical simulations. In this way, the liquid bridge at the particle scale needs to be determined. Yang *et al.* (2012) studied the liquid bridge of even-sized coarse particles and used this theory to derive the vG-liked model. Zhang *et al.* (2013) studied the

liquid bridge of uneven-sized coarse particles, which can be applied to practical engineering problems and theoretical research.

In this study, the relationship between water content, matrix suction and capillary force of liquid bridge is used to analyse the SWCC of uneven-sized coarse particles. The relative size of the sphere, the liquid-solid contact angle and the normalized half-spacing are changed to reflect the various pore structure. The influence of these parameters on the water content, matrix suction and capillary force is discussed. Finally, the SWCC of the compact cubic packing model obtained by the liquid bridge theory is predicted and compared with the prediction reported by the previous study.

2 LIQUID BRIDGE THEORY

When the water in the soil was composed of water in liquid bridges without merging, the liquid bridge between two soil particles can be calculated based on the geometrical relationship. The particles with complex shapes can be simplified as spheres (Mitarai N. *et al.*, 2006). Two complex-shaped particles which contact each other may have spacing when simplified as spheres. Hence the spacing can be used to reflect the roughness of particles (Pietsch *et al.*, 1968). The liquid bridge between two particles can be simplified as a ring which is beneficial for calculation and the results are acceptable (Gillespie *et al.*, 1967). The geometric diagram of the liquid bridge between two soil particles can be shown in Figure 1.

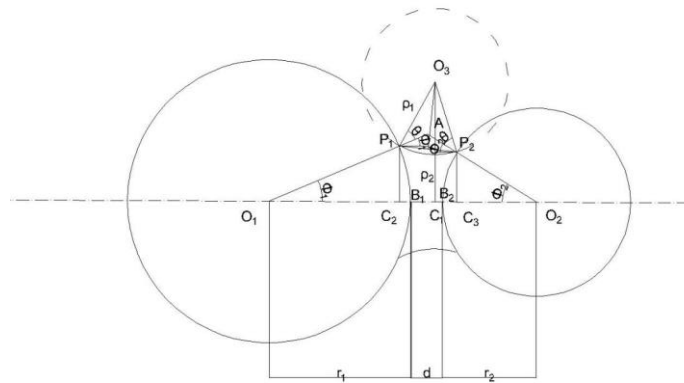


Figure 1. The liquid bridge between uneven-sized coarse particles

This study analyses the liquid bridge between two uneven-sized spheres with the spacing which reflects the roughness. The radius of the two spheres is r_1 and r_2 , the distance between the two spheres is d , and the liquid-solid contact angle is θ . The liquid-solid contact angle of the two spheres is the same due to the same materials. For each fill angle Φ_1 and Φ_2 , the radius of curvature (ROC) ρ_1 , ρ_2 and water content V can be calculated through geometric analysis. Matric suction ψ and capillary force f can be calculated through mechanical analysis.

2.1 Geometric analysis

For each given fill angle Φ_1 , the corresponding fill angle Φ_2 , the radius of curvature ρ_1 , ρ_2 and the water content V can be calculated. The ROC ρ_1 , ρ_2 can reflect the details of liquid bridge morphology which can be used in mechanical analysis. The water content V is one of the main research parameters in this study.

2.1.1 The calculation of fill angle Φ_2

In ΔAP_1P_2 : $\angle AP_1P_2 = \angle AP_2P_1 = \frac{\pi - \Phi_1 - \Phi_2 - 2\theta}{2}$, which means $AP_1 = AP_2$.

To simplify the calculation, the length of AP_1 and AP_2 are regarded as l . Two equations describing the length of AC_1 and C_2C_3 are listed as follows:

$$AC_1: (r_1 + l)\sin\phi_1 = (r_2 + l)\sin\phi_2 \quad (1)$$

$$C_2C_3: (l\cos\phi_1 + l\cos\phi_2) = (r_1(1 - \cos\phi_1) + r_2(1 - \cos\phi_2) + d) \quad (2)$$

The relationship between ϕ_1 and ϕ_2 can be calculated by:

$$\left(\left(r_1 + \frac{d}{2} \right) \tan \frac{\phi_1}{2} \right) = \left(\left(r_2 + \frac{d}{2} \right) \tan \frac{\phi_2}{2} \right) \quad (3)$$

The solution of fill angle ϕ_2 is deduced as:

$$\phi_2 = 2 \arctan \left(\frac{\left(r_1 + \frac{d}{2} \right) \tan \frac{\phi_1}{2}}{\left(r_2 + \frac{d}{2} \right)} \right) \quad (4)$$

2.1.2 The calculation of ROC ρ_1 and ρ_2

The length of C_2C_3 can be described using the horizontal projection of O_3P_1 and O_3P_2 as:

$$C_2C_3: \rho_1(\cos(\phi_1 + \theta) + \cos(\phi_2 + \theta)) = (r_1(1 - \cos\phi_1) + r_2(1 - \cos\phi_2) + d) \quad (5)$$

The solution of ROC ρ_1 is then written as follows:

$$\rho_1 = \frac{(r_1(1 - \cos\phi_1) + r_2(1 - \cos\phi_2) + d)}{(\cos(\phi_1 + \theta) + \cos(\phi_2 + \theta))} \quad (6)$$

By using the length of O_3C_1 , we have:

$$O_3C_1: \rho_1 + \rho_2 = \rho_1 \sin(\phi_1 + \theta) + r_1 \sin\phi_1 \quad (7)$$

Hence the solution of ROC ρ_2 is obtained as follows:

$$\rho_2 = \rho_1 \sin(\phi_1 + \theta) + r_1 \sin\phi_1 - \rho_1 \quad (8)$$

2.1.3 The calculation of water content V

The water content V can be obtained by subtracting the volume of two spherical crowns V_{ss} from the volume of the body of the revolution V_{mp} . The length of O_3C_1 ($\rho_1 + \rho_2$) is regarded as a .

The volume of the body of revolution V_{mp} is obtained through the integral as follows:

$$\begin{aligned} V_{mp} &= \int_{-\rho_1 \cos(\phi_1 + \theta)}^{\rho_1 \cos(\phi_2 + \theta)} \pi (a - \rho_1 \cos\alpha)^2 d(\rho_1 \sin\alpha) = \int_{-\left(\frac{\pi}{2} - (\phi_1 + \theta)\right)}^{\left(\frac{\pi}{2} - (\phi_2 + \theta)\right)} \pi (a - \rho_1 \cos\alpha)^2 \rho_1 \cos\alpha \, d\alpha \\ &= \int_{-\left(\frac{\pi}{2} - (\phi_1 + \theta)\right)}^{\left(\frac{\pi}{2} - (\phi_2 + \theta)\right)} \pi (a^2 \rho_1 \cos\alpha - 2a\rho_1^2 \cos\alpha^2 + \rho_1^3 \cos\alpha^3) \, d\alpha \end{aligned}$$

V_{mp} can be simplified as:

$$\begin{aligned} V_{mp} &= a^2 \rho_1 \pi (\cos(\phi_1 + \theta) + \cos(\phi_2 + \theta)) \\ &- 2a\rho_1^2 \pi \frac{\sin(\phi_1 + \theta) \cos(\phi_1 + \theta) + (\phi_1 + \theta) + \sin(\phi_2 + \theta) \cos(\phi_2 + \theta) + (\phi_2 + \theta)}{2} \\ &+ \rho_1^3 \pi \left(\cos(\phi_1 + \theta) + \cos(\phi_2 + \theta) - \frac{\cos(\phi_1 + \theta)^3}{3} - \frac{\cos(\phi_2 + \theta)^3}{3} \right) \end{aligned} \quad (9)$$

The volume of two spherical crowns V_{ss} is given by the spherical crown volume formula as:

$$V_{ss} = \frac{\pi r_1^3 (3(1 - \cos\phi_1)^2 - (1 - \cos\phi_1)^3)}{3} + \frac{\pi r_2^3 (3(1 - \cos\phi_2)^2 - (1 - \cos\phi_2)^3)}{3} \quad (10)$$

The water content V is calculated as:

$$V = V_{mp} - V_{ss} \quad (11)$$

2.2 Mechanical analysis

Matric suction ψ can be given by the Yang-Laplace equation (Laplace, P.S. 1806) as:

$$\psi = \sigma \left(\frac{1}{\rho_1} - \frac{1}{\rho_2} \right) \quad (12)$$

where σ denotes surface tension.

Capillary force f includes the force of matric suction and the force of surface tension (Simons *et al.* 1994). The matric suction acts on the narrowest section of the liquid bridge, and the surface tension acts on the circumference of the narrowest section of the liquid bridge.

The force of matric suction f_ψ can be written as follows:

$$f_\psi = \psi \pi \rho_2^2 = \left(\frac{1}{\rho_1} - \frac{1}{\rho_2} \right) \pi \rho_2^2 \sigma \quad (13)$$

The force of surface tension f_σ is shown as:

$$f_\sigma = 2\pi \rho_2 \sigma \quad (14)$$

The Capillary force f is calculated as:

$$f = f_\psi + f_\sigma = \left(\frac{1}{\rho_1} + \frac{1}{\rho_2} \right) \pi \rho_2^2 \sigma \quad (15)$$

In practice, there are also effects of gravity and buoyancy. To facilitate the reaction of the rate of particle gravity and capillary force, Mitarai *et al.* (2006) introduced capillary length a_c :

$$a_c = \sqrt{\frac{\sigma}{\rho_l g}} \quad (16)$$

where ρ_l is liquid density.

When the capillary length a_c is smaller than the radius of spheres, the capillary force plays a leading role, and gravity can be ignored. In addition, Willett *et al.* (2000) found that the relative error of considering the influence of buoyancy is less than 0.1% when calculating the capillary force.

2.3 Normalized Results

The normalized results can reflect the essence of the relationship between parameters and water content, matric suction, and capillary force. Here, we introduce the relative size of the sphere n and the average radius R_m as follows for normalization:

$$n = \frac{r_2}{r_1} \quad (17)$$

$$R_m = \frac{(1+n)}{2} r_1 \quad (18)$$

The average of radius R_m is used for Geometric parameters normalization, matric suction and capillary force normalization. Surface tension σ is used for matric suction and capillary force normalization.

The definition of normalized parameters and normalized results are as follows in Table 1.

Table 1. Normalized parameters

Name	symbol	Definition
Normalized Radius r_1	r_1'	$r_1' = \frac{r_1}{R_m} = \frac{2}{1+n}$ (19)
Normalized Radius r_2	r_2'	$r_2' = \frac{r_2}{R_m} = \frac{2n}{1+n}$ (20)
Normalized half-spacing	S	$S = \frac{s}{R_m} = \frac{d}{2R_m}$ (21)
Normalized ROC ρ_1	ρ_1'	$\rho_1' = \frac{\rho_1}{R_m}$ (22)
Normalized ROC ρ_2	ρ_2'	$\rho_2' = \frac{\rho_2}{R_m}$ (23)
Normalized water content	V'	$V' = \frac{V}{R_m^3}$ (24)
Normalized matric suction	ψ'	$\psi' = \psi * \frac{R_m}{\sigma} = \left(\frac{1}{\rho_1} - \frac{1}{\rho_2} \right) R_m = \left(\frac{1}{\rho_1'} - \frac{1}{\rho_2'} \right)$ (25)

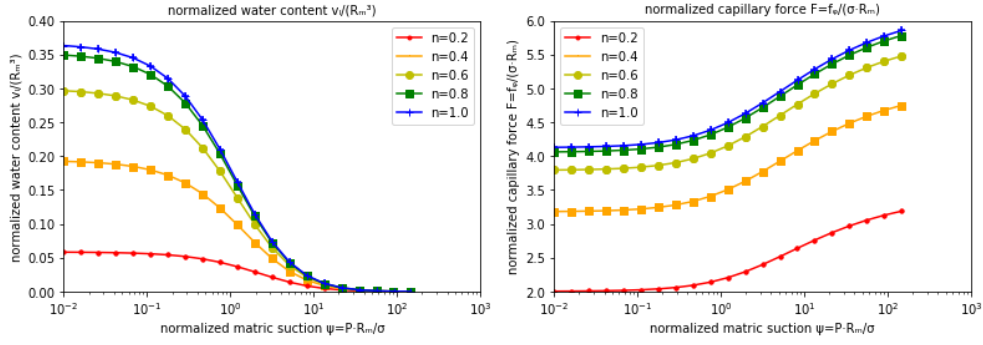
After normalization, three parameters including the relative size of sphere n , the liquid-solid contact angle θ and the normalized half-spacing S reveal the influence of the relative size of two spheres, water and soil mechanical properties and particles roughness on the normalized water content, the normalized matric suction and the normalized capillary force.

3 PARAMETERS ANALYSIS BETWEEN TWO PARTICLES

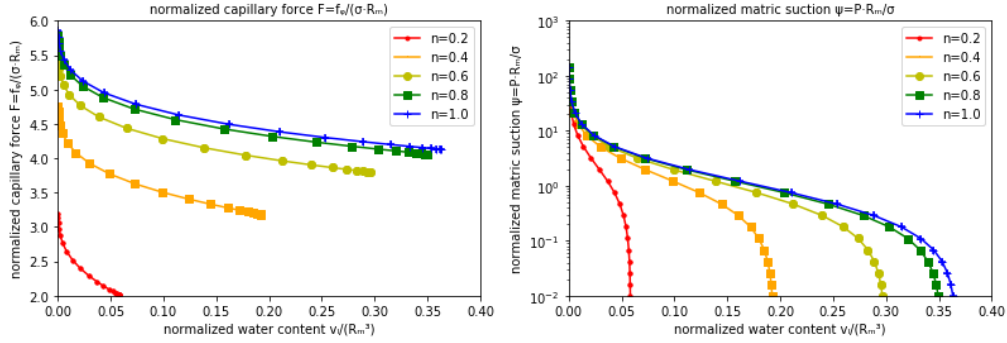
In parameters analysis, we discuss the influences of the relative size of sphere n , the liquid-solid contact angle θ and the normalized half-spacing S on the relationship between water content, matrix suction and capillary force of liquid bridge.

3.1 The relative size of sphere n

In this study, r_1 is larger than r_2 , which means $n \leq 1$. To analyse the relative size of sphere n , we assume that the liquid-solid contact angle θ is fixed at 10° , which means that the contact angle will keep its original value as the water content changes. In addition, we assume that the normalized half-spacing S is 0, which means that there is no spacing and roughness. The influences of the relative size of sphere n on a liquid bridge are shown in Figure 2.



(a) Normalized matrix suction-water content (b) Normalized matrix suction-capillary force

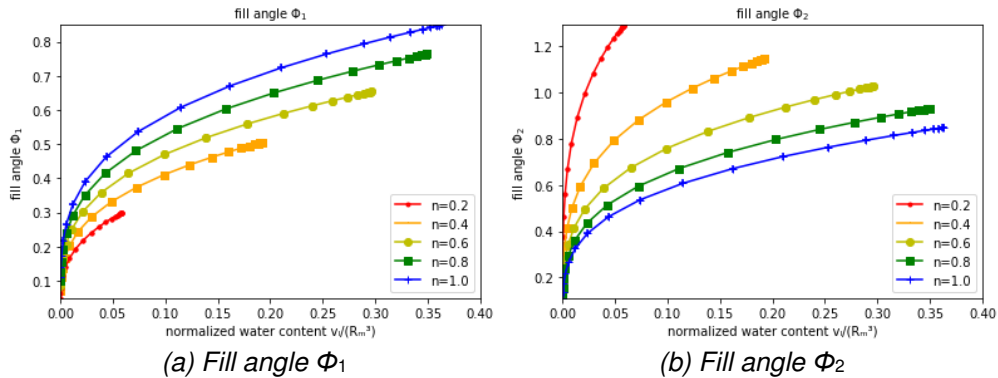


(c) Normalized water content-capillary force (d) Normalized water content-matrix suction

Figure 2. Liquid bridge curve with the different relative size of sphere n ($S=0, \theta=10^\circ$)

As Figure 2 shows, as the relative size of sphere n approaches 1, which means the relative size of two spheres becomes closer, the normalized water content V and the normalized capillary force f increase corresponding to the same normalized matrix suction ψ' , and the normalized capillary force f increases corresponding to the same normalized water content V .

The relationship between the normalized matrix suction ψ' and the normalized water content V can be explained as follows. Eq. (25) shows that the normalized matrix suction ψ' is determined by the normalized ROC ρ_1' and ρ_2' . In Figure 3, for the same normalized water content V , as the size of the small sphere increase, the fill angle of the big sphere Φ_1 increase while the fill angle of the small sphere Φ_2 decreases. Meanwhile, the normalized ROC ρ_1' which reflects the contour of the liquid bridge decreases and the normalized ROC ρ_2' which reflects the thickness of the liquid bridge increases. The decrease in ρ_1' and the increase in ρ_2' lead to the increase of the normalized matrix suction ψ' .



(a) Fill angle Φ_1

(b) Fill angle Φ_2

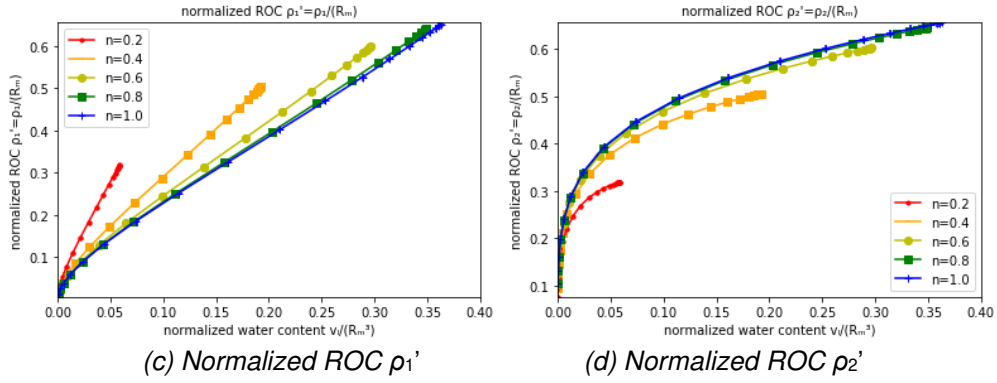


Figure 3. Fill angle and normalized ROC with the different relative size of sphere n ($S=0, \theta=10^\circ$)

With the increase of normalized matrix suction ψ' , the normalized water content V decreases gradually. When the normalized matrix suction ψ' reaches 100, the normalized water content V is almost zero. This conclusion is consistent with Zhang *et al.* (2013). With the increase of normalized matrix suction ψ' , the normalized capillary force \bar{f} also increases gradually.

3.2 The liquid-solid contact angle θ

The relative size of sphere n is fixed as 0.4, and the normalized half-spacing $S=0$. The relationships of the normalized water content, the normalized matrix suction, and the normalized capillary force are displayed as shown in Figure 4.

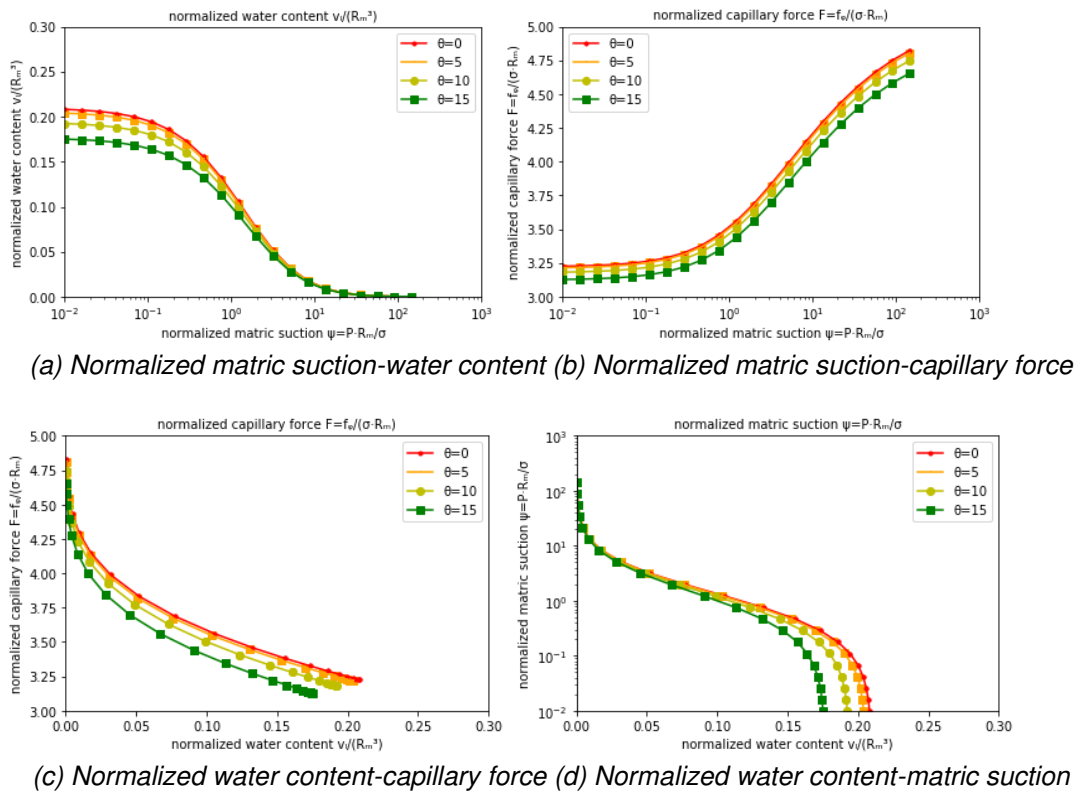


Figure 4. Liquid bridge curve with different liquid-solid contact angle θ ($S=0, n=0.4$)

In Figure 4, as the liquid-solid contact angle θ increases, the normalized water content V and the normalized capillary force f corresponding to the same normalized matrix suction ψ' are reduced. Due to the increase of the liquid-solid contact angle θ , the normalized ROC ρ_1' will increase significantly as Figure 5 shows, while it has little effect on the normalized water content V . Therefore it can be

considered that the normalized ROC ρ_1' increases with the increase of solid-liquid contact angle at the same relative water content V , resulting in the decrease of matrix suction ψ' .

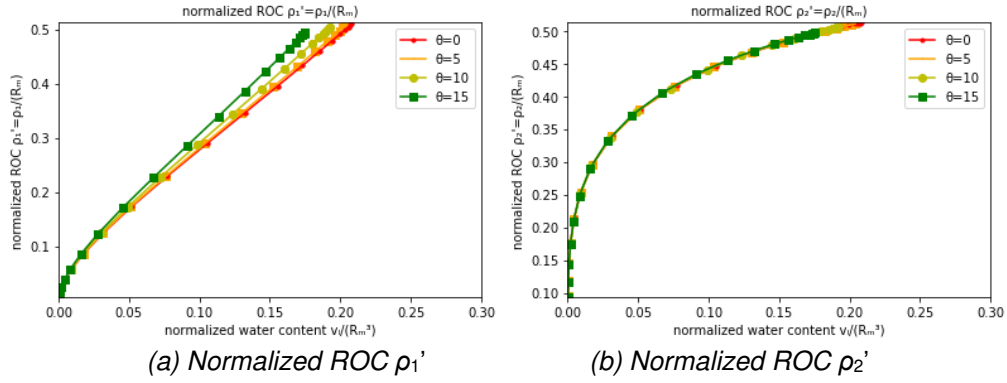


Figure 5. Normalized ROC with different liquid-solid contact angle θ ($S=0, n=0.4$)

3.3 The normalized half-spacing S

The influence of the normalized half-spacing S on the normalized matrix suction-water content, normalized matrix suction-capillary force, normalized water content-capillary force and normalized water content-matrix suction is shown in Figure 6. In this scenario the liquid-solid contact angle is $\theta=10^\circ$ and the relative size of sphere is $n=0.4$.

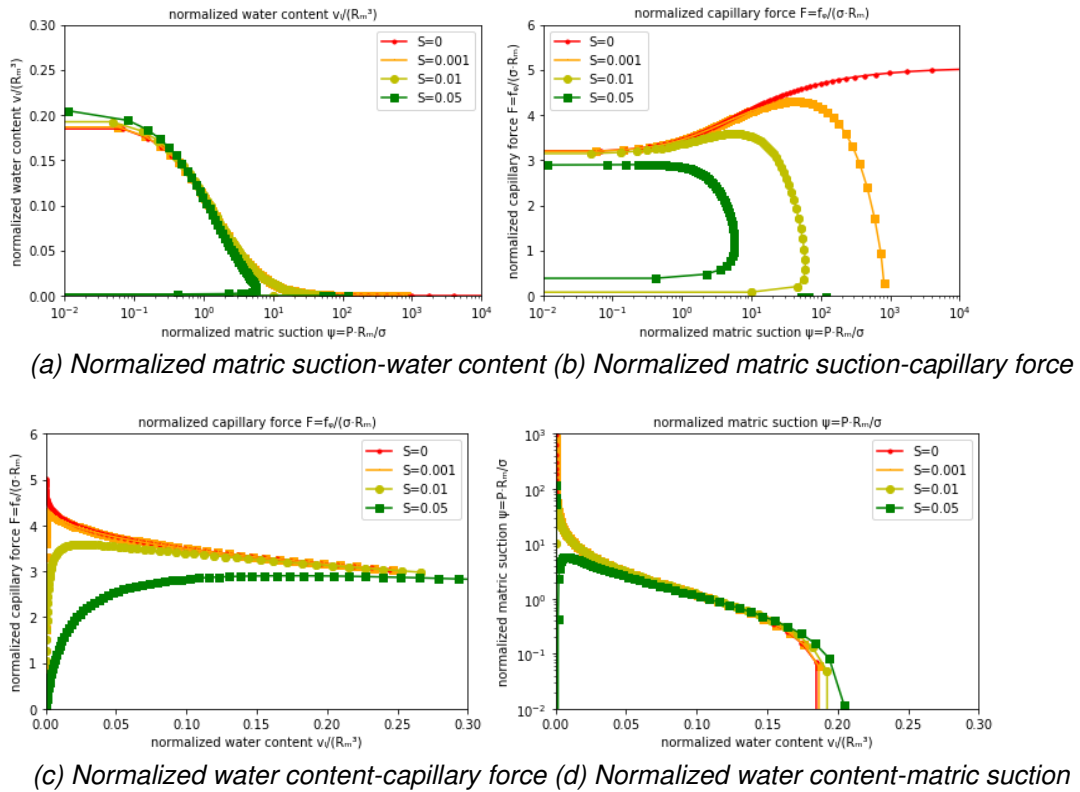


Figure 6. Liquid bridge curve with different normalized half-spacing S ($n=0.4, \theta=10^\circ$)

According to Figure 6, there will be two normalized water content V corresponding to the same matrix suction ψ' if the normalized half-spacing S cannot be ignored. The normalized ROC ρ_1' and ρ_2' increase with the increase in normalized water content V as Figure 7 shows. The increase in ρ_1' leads to the decrease of the matrix suction ψ' while the increase in ρ_2' leads to the increase of the matrix suction ψ' . Hence the increase in ρ_1' and ρ_2' leads to two normalized water content V corresponding to the same matrix suction ψ' . This means the liquid bridge between two spheres with spacing or significant

roughness cannot exist stably if the water content is too low. Molenkamp *et al.* (2003) proposed the smaller normalized water content V corresponding to the same normalized matric suction ψ' is unstable, and the higher one is stable. If we only take the stable solution in consideration, with the growing of the normalized half-spacing S , the stable normalized water content V is on the increase, and the stable normalized capillary force f is on the decrease.

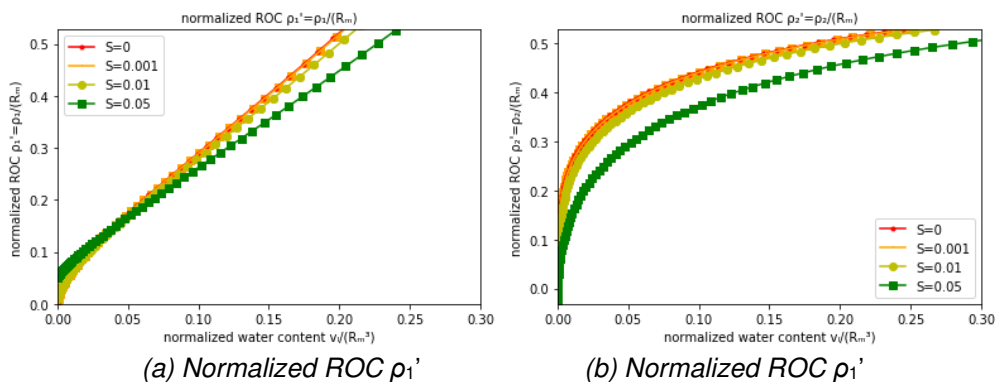


Figure 7. Normalized ROC with different normalized half-spacing S ($n=0.4, \theta=10^\circ$)

4 ANALYSIS OF SOIL PARTICLE ACCUMULATION MODEL

When the water in the soil particle accumulation model is composed of water in the different liquid bridges without merging, the water content of each liquid bridge can be calculated separately. Hence the total water content of the liquid bridge can be calculated. If the film water can be ignored, the total water content of the model can be approximately considered as the total water content of the liquid bridges.

The precise solution of the water content distribution of multiple liquid bridges needs calculating based on the principle of minimum energy. If the influence of gravity, buoyancy and other factors can be ignored, it can be assumed that the matric suction of each liquid bridge on a small scale is the same. The soil-water characteristic curve of the model can be conveniently calculated by the liquid bridge theory.

When calculating SWCC by the liquid bridge theory, the liquid bridge can not get merged, which means the maximum water content is limited. On the other hand, the water in the liquid bridge is much more than the film water, which limits the minimum water content. If the spacing or roughness of two spheres cannot be ignored, the liquid bridge exists unstably if the water content is lower. Water in an unstable liquid bridge should not be considered.

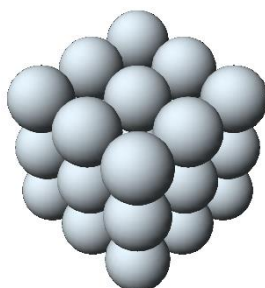


Figure 8. Compact cubic packing model

The compact cubic packing model shows in Figure 8. Each particle has the same size ($n=1$) and has 6 contacts with other intimate contacts ($S=0$). The spacing of face-to-corner particles or cubic diagonal particles is too big so the liquid bridges between these particles are unstable or stable with a low water content which can be ignored. In addition, if the liquid bridges between these particles exist stably and cannot be ignored, these liquid bridges will get merged which means the calculation of SWCC by liquid bridge theory can not be applied. Only intimate contact is considered. The curves of the liquid bridge between even-sized smooth particles are exhibited in Figure 9.

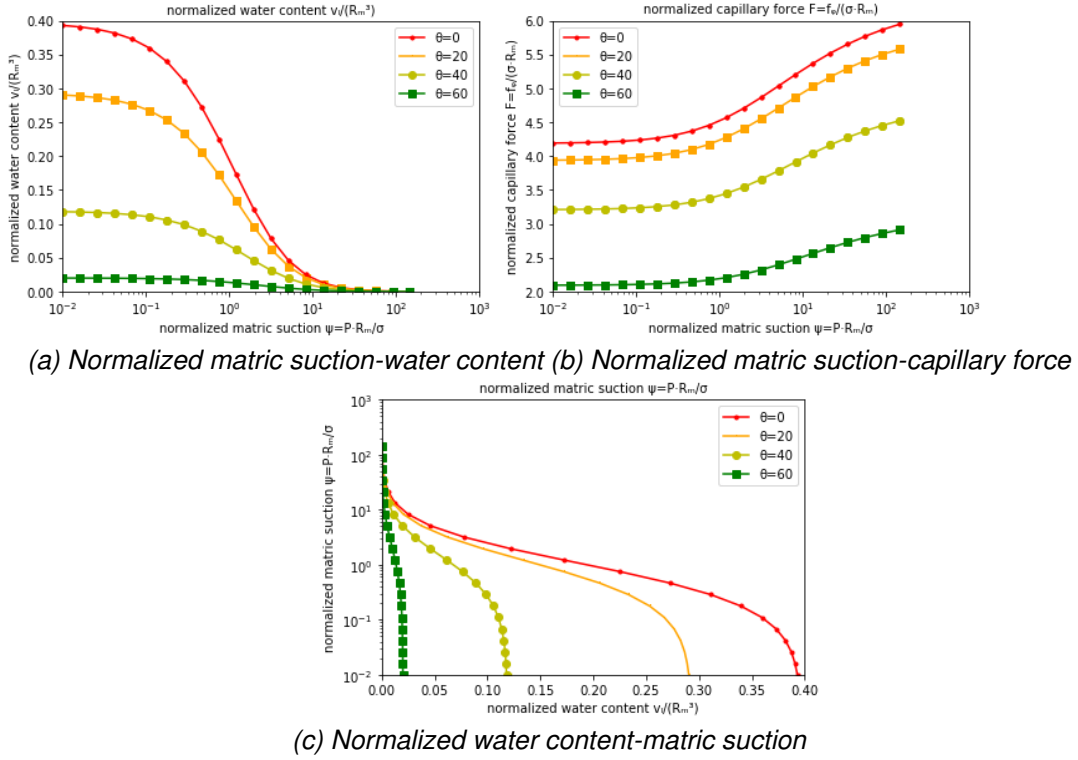


Figure 9. Liquid bridge curve between even-sized smooth particles with different θ ($S=0$, $n=1$)

The porosity of the compact cubic packing model is 0.52. The water content of each particle is 3 times the water content of a liquid bridge between even-sized smooth particles. To avoid liquid bridge merging, the film angle should be less than 45° . Figure 10 shows that, if the liquid-solid contact angle θ is bigger than 20° , the complete SWCC is calculated. If the liquid-solid contact angle θ is too less, the SWCC in high water content can not be calculated because the liquid bridges get merged.

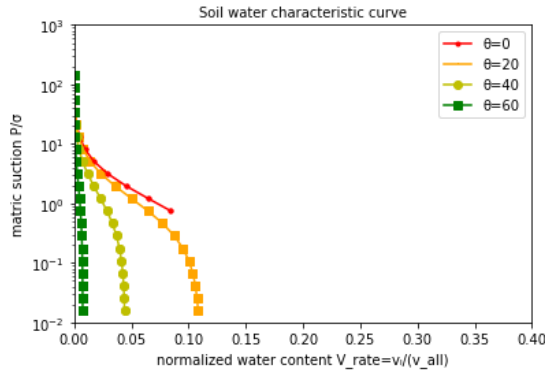


Figure 10. Compact cubic packing model

To verify the theory and results in this study, these results of the simulation are compared with that of the calculations reported by Lu *et al.* 2004. In this case, the radius of the particle r is 1.0 mm, surface tension $\sigma=0.072$ N/m, specific gravity $G_s=2.65$, the liquid-solid contact angle θ is 0° and compact cubic stacking void ratio $e=0.91$. Some figures in the case are describing the relationship between the mass moisture content and the matric suction with different particle sizes in a compact cubic packing model. These curves were given by the approximate equation of water content in the liquid bridge between two even-sized smooth particles by Dallavalle J. M. (1943) as follows.

$$V = 2\pi r^3 \left(\frac{1}{\cos\theta} - 1 \right)^2 \left(1 - \left(\frac{\pi}{2} - \theta \right) \tan\theta \right) \quad (26)$$

The results are shown in Figure 11. The results of these two calculations consistent with each other. Eq. (26) given by Dallavalle J.M. can only describe the liquid bridge between two even-sized particles with no spacing, while Eq. (9-11) can be used to calculate the water content in the liquid bridge between two uneven-sized particles with spacing.

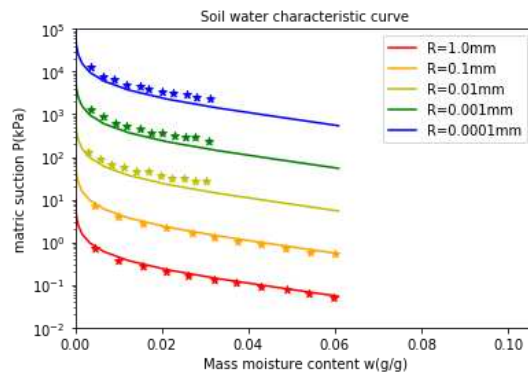


Figure 11. Compact cubic packing model ($\theta=0$, $n=1$)
(The solid lines are the calculation results of liquid bridge theory, and the points are the curve sampling results reported by Lu et al., 2004)

5 CONCLUSIONS

In this study, the soil water characteristic curve of the simple model is calculated based on the analysis of the liquid bridge. This method can provide a theoretical explanation of the measured SWCC data. The effectiveness of this method has been verified by the case in unsaturated soil mechanics.

The uneven-sized coarse particle with the same materials is analysed. The parameter analysis shows that with the increase of the small sphere or the decrease of the liquid-solid contact angle θ , the normalized water content V' and the normalized capillary force f' increase corresponding to the same normalized matric suction ψ' . These are mainly due to the decline of ROC ρ_1 and/or the increase of ROC ρ_2 . It also shows that when the spacing cannot be ignored, there may be two normalized water content corresponding to the same normalized matric suction ψ' . The higher solution of water content is stable.

This method reported by this study can be used in the calculation of SWCC in simple models. In this study, the compact cubic packing model is analysed with the same matric suction in each liquid bridge assumption. The result is consistent with the results calculated in the previous study, which proves the accuracy of this method.

It should be noted that this method has some limitations. The water content has limitations since the liquid bridge should be stable and not merge with other liquid bridges. The soil-liquid contact angle is a constant in this study while the angle may change with water content. In future research, the theoretical calculation method of SWCC in a wider range of water content and the change of solid-liquid contact Angle with water content can be studied.

6 ACKNOWLEDGEMENTS

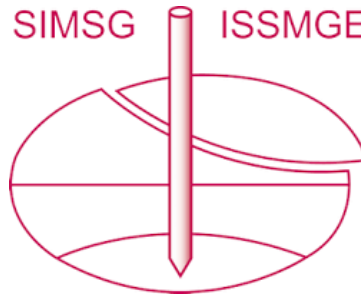
The National Natural Science Foundation of China (51979144, 42207002), the Beijing Natural Science Foundation (8224092) and the CRSRI Open Research Program (CKWV20221013/KY) supported this work.

REFERENCES

- Dallavalle, J.M. (1948). Micromeritics: the technology of fine particles.
Gillespie, T., Settineri, W. J. (1967). The effect of capillary liquid on the force of adhesion between spherical solid particles. Journal of Colloid & Interface Science, 24(2), 199-202.

- Lu, N., & Likos, W. J. (2004). *Unsaturated soil mechanics*. J. Wiley.
- Laplace, P.S. (1806). *Mecanique Celeste*, suppl. 10th vol. English translation reprinted by Chelsea, New York
- Mehrotra V. P., Sastry K. V. S. (1980). Pendular bond strength between unequal-sized spherical particles. *Powder Technology*, 25(2), 203-214.
- Miller, C. J., Yesiller, N., Yaldo, K. and Merayyan, S. (2002). Impact of soil type and compaction conditions on soil water characteristic. *Journal of Geotechnical & Geoenvironmental Engineering*, 128(9), 722–742.
- Mitarai, N., Nori, F. (2006). Wet granular materials. *Advances in Physics*, 55, 1 - 45.
- Molenkamp F, Nezomi A H. (2003). Interactions between two rough spheres, water bridge and water vapour. *Geotechnique*, 53(2), 255-264.
- Ng, C.W., Pang, Y.W. (2000). Influence of Stress State on Soil-Water Characteristics and Slope Stability. *Journal of Geotechnical and Geoenvironmental Engineering*, 126, 157-166.
- Orr, F.M., Scriven, L.E., and Rivas, A.P. (1975). Pendular rings between solids: meniscus properties and capillary force. *Journal of Fluid Mechanics*, 67, 723 - 742.
- Pietsch, W. (1968). Tensile Strength of Granular Materials. *Nature*, 217, 736-737.
- Simons, S.J., Seville, J.P., and Adams, M.J. (1994). An analysis of the rupture energy of pendular liquid bridges. *Chemical Engineering Science*, 49, 2331-2339.
- Genuchten, V., Th., M. (1980). A closed-form equation for predicting the hydraulic conductivity of unsaturated soils. *Soil Science Society of America Journal*, 44, 892-898.
- Willett C D, Adams M J, Johnson S A, et al. (2000). Capillary bridges between two spherical bodies. *Langmuir*, 16(24), 9396-9405.
- Yang S, Lu T H. (2012). Study of soil-water characteristic curve using microscopic spherical particle model. *Pedosphere*, 22(1), 103-111.
- Zhang Z, LIU F Y, Zhang G P, Zheng F. (2013). Microscopic hydraulic behavior from the interactions between uneven-sized wet particles and liquid bridge. *Journal of Hydraulic Engineering*, 44(7), 810-817.

INTERNATIONAL SOCIETY FOR SOIL MECHANICS AND GEOTECHNICAL ENGINEERING



This paper was downloaded from the Online Library of the International Society for Soil Mechanics and Geotechnical Engineering (ISSMGE). The library is available here:

<https://www.issmge.org/publications/online-library>

This is an open-access database that archives thousands of papers published under the Auspices of the ISSMGE and maintained by the Innovation and Development Committee of ISSMGE.

The paper was published in the proceedings of the 9th International Congress on Environmental Geotechnics (9ICEG), Volume 3, and was edited by Tugce Baser, Arvin Farid, Xunchang Fei and Dimitrios Zekkos. The conference was held from June 25th to June 28th 2023 in Chania, Crete, Greece.